

Analysis of the Cyclic Stress Ahead of Short Cracks at $R = -1$

Mauro Madia

Dipartimento di Meccanica, Politecnico di Milano, I-20156 Milano, Italy
mauro.madia@polimi.it

Keywords: small cracks; asymptotic fields; constraint effect; FEA.

Abstract. The present work addresses the problem of the correct assessment of the stress field ahead of small cracks in specimens subjected to fatigue tests. Finite element analysis were carried out on cracked specimens in order to derive the stress field at threshold level. The stress state was analysed in light of the governing equations of the asymptotic fields; in particular the J - A_2 theory proved to be an effective tool for characterizing the effective state of stress at threshold level ahead of the crack tip taking into account the cyclic properties of the material.

Introduction

The discussion about the resistance against initiation of ductile crack growth and crack propagation covered the last 50 years, in particular it is well known that it depends on the loading conditions as well as the overall geometrical and boundary configurations of the tested specimens or components.

The main issue is that the measure of the load intensity, given in terms of K (in case of linear elastic fracture mechanics) or J (in case of non-linear fracture mechanics), does not provide a sufficient condition in order to reproduce accurately the stress-strain field ahead of the crack tip. An intensive and extensive discussion arose with the purpose to find a better characterization of the near-tip crack fields, which is known as the so-called *constraint effects*. As the only value of K or J proved to be not satisfactory to reproduce the state of stress at the crack tip [1-3], the general agreement between the authors was to enhance the basic solutions by introducing a second parameter, which could quantify the level of constraint at the crack tip.

The idea of a two-parameter representation of the crack-tip fields and the constraint effects in fracture mechanics were discussed in the 90's, mainly due to the development of the finite element codes to analyze more general three-dimensional local fields.

Many authors [4-7] stated the possibility to describe the stress field and the stress triaxiality ahead of the crack tip on the basis of J and T -stress values. In particular, they found that positive values of the T -stress do not effect the value of the triaxiality, whereas the compressive T -stress reduces the triaxiality of the stress state within the plastic zone.

A relevant contribution to the characterization of the crack-tip fields was given by O'Dowd and Shih [8,9], who introduced the concept of Q -stress as second parameter. They found that the parameter Q is responsible for the stress distribution and maximum stress ahead of the crack tip, whereas the role of J is to set the size scale over which the large stress and large strains develop. The main limitation of the so-called J - Q theory is that the second parameter is constant, thus yielding a trivial translation of the HRR field and a poor estimation of the stress field far from the crack tip.

An important enhancement in the representation of the crack-tip fields is represented by the J - A_2 theory [10]. The authors described the stress field with an asymptotic series solution and they demonstrated that, under plane strain conditions and in case of low or moderate hardening materials, the first three terms of the series can be used to characterize the crack-tip mechanics fields over larger distances from the crack tip for a wide number of specimen geometries and constraint levels. The main enhancement of the J - A_2 theory, in comparison with the other two-parameters solutions, is the dependence of the higher order terms by the radial distance r from the crack tip. This feature

allows to reproduce well the stress field even in 3D configurations, all along the crack front up to the free surface.

The important point is that all the approaches were developed on the basis of the tensile monotonic properties of the material, moreover, most of the contributions which can be found in the literature deal with materials commonly employed for lightweight structures, such as aluminum alloys. Previous researches by the author [11,12] showed the importance of considering the cyclic properties of the material to predict the fatigue strength and thresholds for steel components. In the present study, the asymptotic solutions were successfully applied to the case of two steels for structural applications, taking into account the cyclic properties of the materials.

Experimental characterization of the materials

The materials under investigation were two mild steels: the first one is named E355SR, according to the European standard EN 10305-1, and it is used in the production of tubes for structural applications, whereas the second one is named A1N and it is employed in the construction of railway axles. A series of experimental tests were carried out with the purpose to characterize the basic mechanical properties and the fatigue behaviour of the materials [11,12]: monotonic tensile tests, low cycle fatigue tensile tests, fatigue tests on smooth and micro-notched specimens. The basic monotonic and cyclic properties are reported in Table 1.

Table 1. Basic mechanical properties of the materials [11,12].

Material	E [MPa]	$R_{p0.2}$ [MPa]	UTS [MPa]	E_{cyc} [MPa]	$R_{p0.05cyc}$ [MPa]	$R_{p0.2cyc}$ [MPa]
E355SR	203000	585	685	204000	365	450
A1N	197500	388	591	200000	288	364

Fatigue tests were carried out on hourglass smooth and micro-notched specimens (see Fig. 1.a) in order to define the fatigue limits σ_w of the considered materials and their sensitivity to defects and inclusions. The tests for both the steels were performed at $R = -1$. The stair case sequences were used and the specimens were considered run-out if they survived $12 \cdot 10^6$ fatigue cycles. The defect dimensions and the results of the fatigue tests are summarized in Table 2.

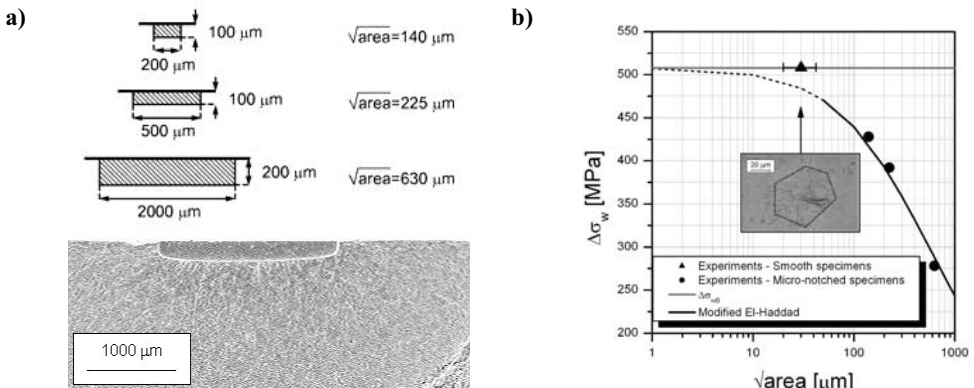


Fig. 1. Fatigue tests for the A1N steel [12]: a) dimensions of the micro-notches and defect with $\sqrt{area} = 630 \mu m$ observed at the SEM; b) Kitagawa-Takahashi diagram.

It is of some importance to remark that the fatigue limit on smooth specimens at $R = -1$ resulted to be $\sigma_{w0,R=-1} = 355$ MPa for the E355SR steel and 260 MPa for the A1N steel, which are very close to the $R_{p0,05cyc}$.

The fatigue limit data for both the steels were interpolated with the modified El-Haddad relationship [13]:

$$\Delta\sigma_w = \Delta\sigma_{w0} \sqrt{\frac{\sqrt{area_0}}{\sqrt{area} + \sqrt{area_0}}} \quad (1)$$

where $\sqrt{area_0}$ is the El-Haddad parameter. The relationship between $\Delta\sigma_w$ and \sqrt{area} , the so-called Kitagawa-Takahashi diagram, is presented in Fig. 1.b for the A1N steel.

The upper part of the line defining the modified El-Haddad model is dashed because this kind of relationship underestimates the fatigue limits in case of smooth specimens, as the fatigue strength of the smooth pieces is characterized by non-propagating cracks (see Fig. 1.b, [12]).

Table 2. Fatigue limit tests [11,12].

Material	Defect dimension \sqrt{area} [μm]	Defect type	$\sigma_w/\sigma_{w0,R=-1}$	Stress ratio
E355SR	Smooth	-	1	-1
	150	Round	0.84	-1
	630	Narrow	0.52	-1
A1N	Smooth	-	1	-1
	140	Narrow	0.82	-1
	225	Narrow	0.75	-1
	630	Narrow	0.53	-1

Finite element analysis

In order to evaluate the state of stress ahead of the defects, finite element analysis (FEA) were carried out by means of the general purpose commercial code ABAQUS® [14]. Several models were implemented according to the different geometric and load configurations, both 2D and 3D models were employed to study the stress-strain state at the crack tip. In particular the 2D models were useful to characterize the limit condition of pure plane strain, whereas 3D models were used to study the stress variation along the crack front of the defects.

The definition of the crack-tip fields needs a high resolution of the state of stress over the plastic region ahead of the crack tip, thus requiring a highly refined mesh around and along the crack front. To this aim, the sub-modeling technique was employed in order to reduce the computational effort (see Fig. 2). It was also taken advantage of all the possible symmetries.

The models employed isoparametric second-order elements with reduced integration due to their ability to capture the stress concentrations reducing the running time, especially in three dimensions.

The load conditions applied to the models were in the same range as the experimental tests, in particular, the range was chosen close to the fatigue limits at $R = -1$.

The most important point to be discussed is about the material model adopted in the finite element calculations. As previously mentioned, the tensile cyclic properties of the materials were

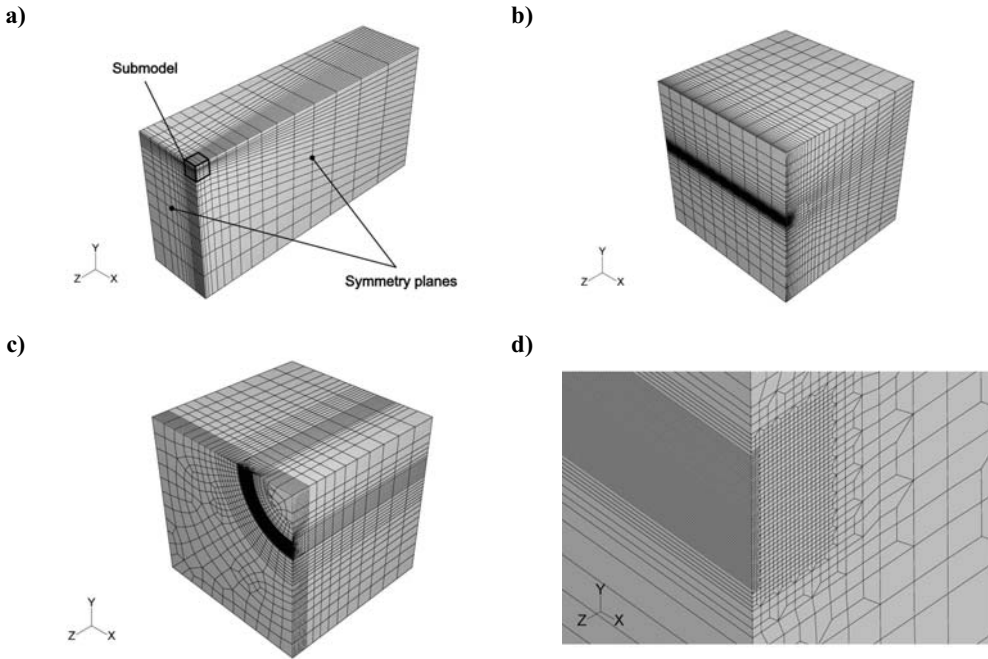


Fig. 2. Finite element models: a) global model of the specimens used in the fatigue tests; b) sub-model of a narrow defect; c) sub-model of a round defect; d) magnification of the mesh employed at the crack front in the sub-models.

used, in particular the material behaviour was modeled by the well-known Ramberg-Osgood relationship (deformation theory of plasticity) [14]:

$$E_{cyc} \varepsilon = \sigma + \alpha \left(\frac{|\sigma|}{\sigma_0} \right)^{n-1} \sigma \quad (2)$$

where the values of the parameters for each material are given in Table 3. It's worth noting that both materials are moderate hardening materials ($n \geq 3$), moreover the yield limit was given in terms of $R_{p0.005cyc}$, which represents the cyclic linear elastic limit.

Table 3. Parameters for the Ramberg-Osgood relationship [11,12].

Material	n	σ_0 [MPa]	α
E355SR	6.620587	250	0.040385
A1N	5.935669	195	0.050659

Reconstruction of the stress field ahead of the crack tip by local parameters

The results of the finite element calculations were compared with the analytical representations of the crack-tip fields. To this aim, of particular interest were the evaluations of the J -integral and T -stress along the crack front, together with the assessment of the second parameter.

J-Q theory. The expression of the *J-Q* theory was proposed by O’Dowd and Shih [8,9] in the following form with reference to cylindrical coordinates:

$$\sigma_{\theta\theta} = (\sigma_{\theta\theta})_{Ref} + Q\sigma_0, \quad Q = \frac{(\sigma_{\theta\theta})_{FEA} - (\sigma_{\theta\theta})_{Ref}}{\sigma_0} \quad \text{at } \theta = 0 \text{ and } r = \frac{2J}{\sigma_0} \quad (3)$$

where $(\sigma_{\theta\theta})_{Ref}$ is the reference solution (HRR) and σ_0 is the cyclic linear elastic limit.

Fig. 3.a shows the results about a three-dimensional narrow defect with $\sqrt{area} = 950 \mu\text{m}$ and applied stress range $\Delta\sigma = 400 \text{MPa}$, considering the cyclic properties of the E355SR steel. It appears clear that the *J-Q* theory is able to provide reliable results just at the crack tip, where the stress field becomes singular, even though it represents an enhancement in comparison to the HRR reference solution (also reported in Fig.3.a). In particular the difference with the finite element data can be considered negligible only up to a distance $r\sigma_0 / J = 5$, which conforms with the literature [8,9]. In general, as all the models showed such a trend, it can be stated that the simple *J-Q* theory is not able to describe the state of stress all over the plastic region ahead of the crack front.

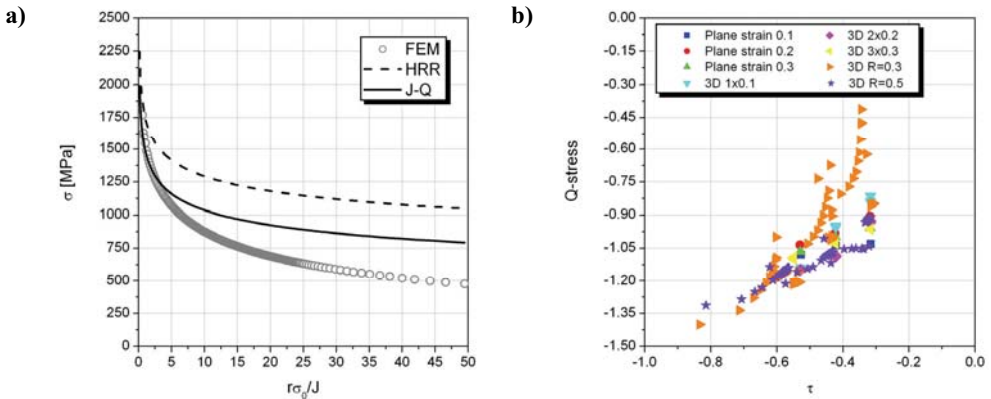


Fig. 3. Application of the *Q*-stress concept to the defects in E355SR steel: a) state of stress at the middle plane of a three-dimensional narrow defect with $\sqrt{area} = 950 \mu\text{m}$ and applied stress range $\Delta\sigma = 400 \text{MPa}$; b) relationship between the *Q*-stress and the *T*-stress.

The numerical analysis of the defects showed that the extension of the plastic region ahead of the crack front keeps quite small, which means that SSY conditions are achieved at the crack tip of defects subjected to threshold load conditions. This finding allowed to study the possible relationship between the *Q*-stress and the *T*-stress, which has a great effect on the stress triaxiality at the crack tip. In particular, already Wang [7] and O’Dowd and Shih [8,9] showed a fair relationship between the parameters (the parameter $\tau = T / \sigma_0$ was used instead of the *T*-stress). The results of the present work, reported in Fig. 3.b, show a poor correlation between the parameters, especially in case of round defects.

J-A₂ theory. It was already stressed in the foregoing that the main reason of the bad approximation given by the *J-Q* theory can be explained by the structure of the stress expression itself, as the second term provides just a pure translation of the HRR solution. By the results available in literature and the ones showed in Fig. 3.a, it’s understood that there exists also a difference in shape between the HRR field and the real field derived by the finite element calculations. This means that it’s necessary to employ a theory including higher order terms, which are vanishingly small close to

the crack tip (where the HRR solution is dominant), but the contribution of which becomes more and more important up to the boundary of the plastic region (where the HRR solution proves to overestimate the stress field).

An important contribution in this direction was given by Yang, Chao and Sutton [10] who proposed the asymptotic solution named $J-A_2$:

$$\frac{\sigma_{ij}(r, \theta)}{\sigma_0} = \left(\frac{J}{\alpha \sigma_0 \varepsilon_0 I_n L} \right)^{\frac{1}{n+1}} \left[\left(\frac{r}{L} \right)^{-\frac{1}{n+1}} \tilde{\sigma}_{ij}^{(1)}(\theta) + A_2 \left(\frac{r}{L} \right)^{s_2} \tilde{\sigma}_{ij}^{(2)}(\theta) + A_2^2 \left(\frac{r}{L} \right)^{s_3} \tilde{\sigma}_{ij}^{(3)}(\theta) \right] \quad (4)$$

in which the values of $\tilde{\sigma}_{ij}^{(1)}(\theta)$, $\tilde{\sigma}_{ij}^{(2)}(\theta)$, $\tilde{\sigma}_{ij}^{(3)}(\theta)$, s_2 and s_3 are reported in tables for various strain hardening exponents n [15]. It's worth noting that the asymptotic solution depends only on J , A_2 and material properties.

An important point to be discussed is the value of the characteristic length L which appears in Eq. 4. In the literature it is often defined as the typical dimension of the specimen or as the crack dimension, but in the present work it was set equal to J/σ_0 because this quantity is representative of the plastic zone extension ahead of the crack tip. In fact the plastic zone size is strictly correlated to the stress magnitude at the crack tip (J) as well as to the strength properties of the material (σ_0).

Another important issue is the assessment of the constraint parameter A_2 . The original proposal [10] was to use a point-matching technique as it was used in the calculation of the Q -stress. In order to avoid any mesh dependence or sensitivity, Nikishkov *et al.* [16] developed another technique based on a least-square fitting procedure in the region $1 < r\sigma_0/J < 5$. This approach was applied also in the present research, moreover it was found that A_2 is slightly dependent on the fitting range.

Some important results about the A1N steel are presented in Fig. 4. As previously mentioned, the entity of the load applied to each defect was about its fatigue limit, which means that it was studied the state of stress for different defect dimensions moving along the modified El-Haddad model. Fig. 4 demonstrates that the $J-A_2$ theory is able to reproduce the stress distribution ahead of the crack tip for each defect at its fatigue limit. The most important aspect, which distinguishes the $J-A_2$ theory from the $J-Q$ theory, is that the approximation by the three terms series keeps its validity up to the boundary of the plastic region.

Another relevant issue was to perform the analysis at remote stress levels far from the fatigue limits of the defects, in order to test the validity of the $J-A_2$ theory in case of lower and larger plasticity at the crack tip. Fig. 5 shows the results of the analysis about a narrow defect in E355SR steel with $\sqrt{area} = 630 \mu\text{m}$. In particular, the analytical approximation proves to be consistent with the finite element data all over the plastic region in case of lower loads (about 25% less than the fatigue limit), whereas in case of higher loads (about 30% more than the fatigue limit) it appears to underestimate the stresses at the boundary of the plastic region. Nevertheless, the $J-A_2$ theory can be employed both in case of contained and large plasticity.

In a similar fashion as the $J-Q$ theory, it was studied whether the second parameter (A_2) could be correlated to the T -stress, or not. The correlation was studied for both materials, for each defect size and load condition, and at each point along the crack front. It's of some importance to recall that the materials are characterized by a similar hardening exponent, but they have different cyclic linear elastic limit σ_0 , which means that, for a given T -stress, the materials have different τ values. The whole data (see Fig. 6), derived by the finite element calculations, show a good correlation between the parameters.

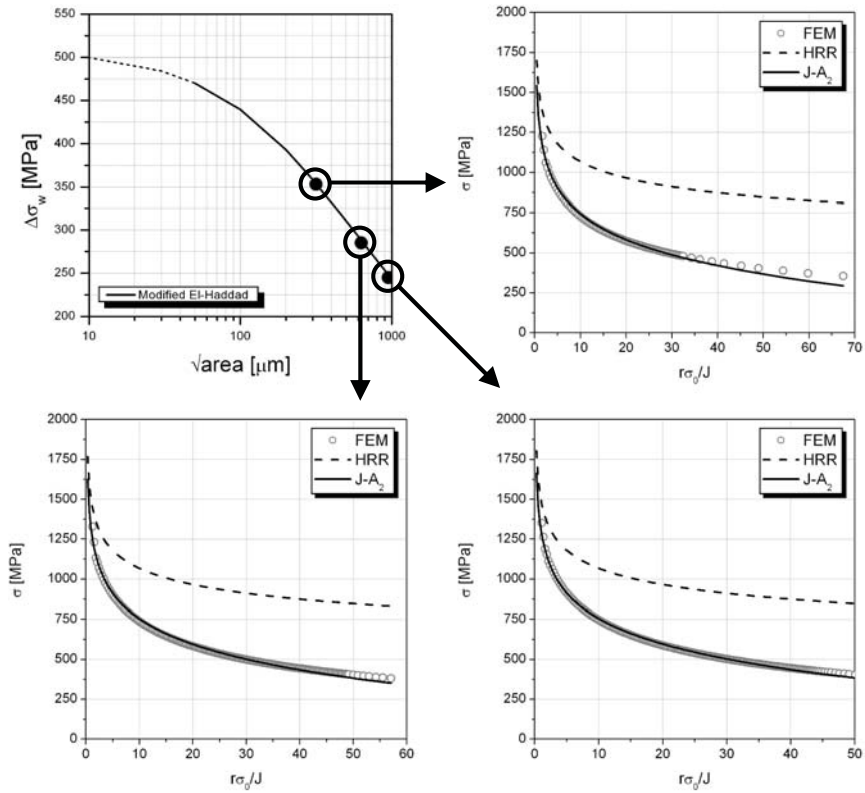


Fig. 4. Application of the $J-A_2$ theory to the reconstruction of the state of stress of the narrow defects in AlN steel subjected to their fatigue limits.

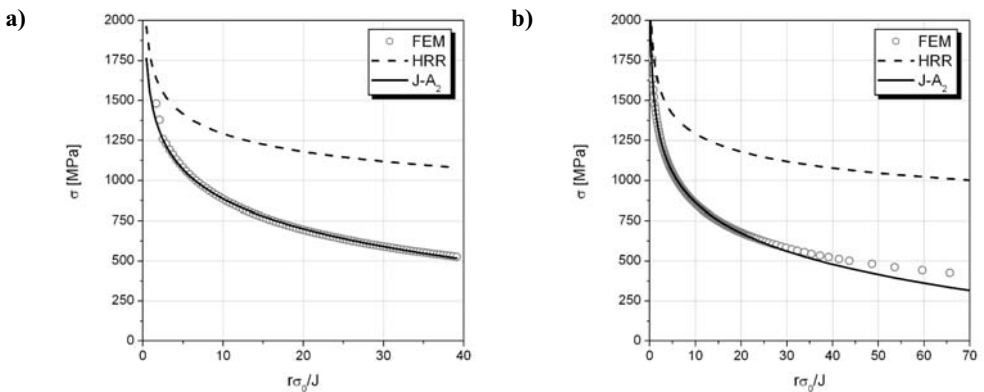


Fig. 5. Application of the $J-A_2$ theory to a defect in E355SR steel with $\sqrt{\text{area}} = 630 \mu\text{m}$: a) applied stress range $\Delta\sigma = 300 \text{ MPa}$; b) applied stress range $\Delta\sigma = 500 \text{ MPa}$.

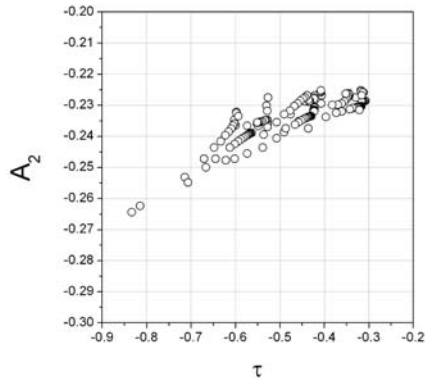


Fig. 6. Correlation between A_2 and $\tau = T/\sigma_0$ for all the finite element analysis.

Acknowledgements

This work is part of the research developed within the Ph.D. activity, under the supervision of Prof. Stefano Beretta at Politecnico di Milano, Dipartimento di Meccanica.

References

- [1] S.J. Larsson and A.J. Carlsson: J. Mech. Phys. Solids Vol. 21 (1973), p. 263-277.
- [2] J.W. Hutchinson: J. Mech. Phys. Solids Vol. 16 (1968), p. 13-31.
- [3] J.R. Rice and G.F. Rosengren: J. Mech. Phys. Solids Vol. 16 (1968), p. 1-12.
- [4] C. Betegon and J.W. Hancock: J. Appl. Mech. Vol. 58 (1991), p. 104-110.
- [5] A.M. Al-Ani and J.W. Hancock: J. Mech. Phys. Solids Vol. 39 (1991), p. 23-43.
- [6] Z.Z. Du and J.W. Hancock: J. Mech. Phys. Solids Vol. 39 (1991), p. 555-567.
- [7] Y.Y. Wang, in: ASTM STP 1171, Philadelphia (1993).
- [8] N.P. O'Dowd and C.F. Shih: J. Mech. Phys. Solids Vol. 39 (1991), p. 989-1015.
- [9] N.P. O'Dowd and C.F. Shih: J. Mech. Phys. Solids Vol. 40 (1992), p. 939-963.
- [10] S. Yang, Y.J. Chao and M.A. Sutton: Eng. Fract. Mech. Vol. 45 (1993), p. 1-20.
- [11] S. Beretta, M. Carboni and M. Madia: J. ASTM Int. Vol. 3 (2006), p. 1-11.
- [12] S. Beretta, M. Carboni and M. Madia, in: Proceedings of Material Models, Hamburg, Germany (2007). Submitted in extended version to Eng. Fract. Mech.
- [13] S. Beretta, in: Proceedings of the 14th European Conference on Fracture (ECF14), Cracow, Poland (2002).
- [14] ABAQUS ver.6.5: *Reference Manual* (2005).
- [15] Y.J. Chao and L. Zhang: *Tables of plane strain crack tip fields: HRR and higher order terms*, Columbia (1997).
- [16] G.P. Nikishkov, A. Bruckner-Foitz and D. Munz: Eng. Fract. Mech. Vol. 52 (1995), p. 685-701.